



## Full factorial study on specific cutting forces in tangential turning of 42CrMo4 steel shafts

István Sztankovics \*  0000-0002-1147-7475

University of Miskolc, Institute of Manufacturing Science, H-3515 Miskolc, Egyetemváros

### ABSTRACT

This study investigates the cutting force characteristics in tangential turning of 42CrMo4 alloy steel using a full factorial experimental design. The aim is to evaluate how cutting speed, feed per revolution, and depth of cut influence the tangential (major cutting force), axial (feed directional force), and radial (thrust force) components, along with their corresponding specific cutting forces. Experimental work was carried out on a hard turning center using tangential turning tooling. Forces were measured with a three-component dynamometer. Eight experimental setups were defined based on combinations of cutting parameters. For each, the three force components and their corresponding specific cutting forces were determined. Polynomial equations were derived to model the influence of the input parameters. The results show that feed and depth of cut significantly increase force magnitudes, while higher cutting speed tends to reduce the major cutting force. Specific cutting forces decrease with larger chip cross-sections, indicating more efficient cutting. However, the specific thrust force shows a more complex response, influenced by chip flow and radial engagement. The study contributes to understanding cutting mechanics in tangential turning and supports optimization of high-feed machining strategies for hardened steels.

### ARTICLE INFO

Received: 22 June 2025

Revised: 15 August 2025

Accepted: 24 August 2025

### KEYWORDS:

Cutting force;  
Design of experiments;  
Force measurement;  
Specific cutting force;  
Tangential turning.

\*Corresponding author's e-mail:  
istvan.sztankovics@uni-miskolc.hu

### 1. INTRODUCTION

Cutting forces are among the most fundamental parameters in machining science, as they directly influence tool wear, energy consumption, surface integrity, dimensional accuracy, and overall process efficiency [1]. In turning, the cutting process involves the interaction between a cutting tool and a rotating workpiece, where material removal occurs through shear deformation of the chip. This process generates forces that act in three principal directions: the tangential (or main cutting) force, which is responsible for the majority of energy input into the cutting zone; the feed force, which resists the advancement of the tool along the feed direction; and the radial force, which tends to deflect the tool away from the workpiece surface. Understanding the magnitude and variation of these forces is essential for predicting machining performance, avoiding excessive tool deflection, preventing chatter, and ensuring that the machine–tool–workpiece system operates within safe limits [2,3].

The measurement and analysis of cutting forces are not only vital for mechanical understanding but also for process optimization. With the advancement of modern manufacturing requirements, especially in the production of high-performance components such as shafts, gears, and precision fittings, the need for accurate cutting force data has grown. It enables engineers to make informed decisions regarding tool geometry, cutting parameters, coolant application, and process strategies to meet strict tolerance requirements while controlling cost and energy usage [4,5].

A particularly useful way to interpret force measurements is through the concept of specific cutting forces [6,7]. Unlike raw cutting force values, which depend on the size of the uncut chip cross-section, specific cutting forces are normalized by the chip cross-sectional area. This normalization allows for a more basic representation of the machinability under given cutting conditions. Specific cutting forces represent the energy needed to remove a unit volume of material and provide a direct link between the

physical properties of the workpiece material, the cutting tool geometry, and the process parameters [8,9]. They serve as a foundation for empirical machining models, tool life prediction formulas, and computer-aided process planning.

From a design and production perspective, lowering specific cutting forces is advantageous for several reasons. Firstly, lower values indicate reduced energy consumption, which directly impacts the sustainability of the machining process and reduces production costs. Secondly, they can lead to lower tool wear rates, extending tool life and decreasing tool replacement frequency. Thirdly, reduced forces minimize mechanical loads on the spindle, feed drives, and workpiece, thereby improving dimensional stability and surface finish. For these reasons, research in machining continually seeks alternative cutting methods, tool designs, and parameter settings that can achieve the same or improved productivity with lower specific cutting forces [10,11].

One approach to lowering cutting forces is through alternative turning methods that depart from conventional longitudinal feeding. While conventional turning advances the cutting tool parallel to the workpiece axis, alternative feed directions – such as tangential or oblique turning – alter the engagement geometry between tool and workpiece. These methods can change chip formation mechanics, redistribute cutting loads, and potentially improve tool–chip contact conditions [12,13]. Such modifications may lead to reduced force components, particularly in high-feed machining scenarios, and can also have beneficial effects on surface geometry and tool life. Tangential turning has emerged as a promising method in this regard. In tangential turning, the feed direction is arranged tangentially to the machined surface rather than along the workpiece axis [14,15]. This results in a cutting engagement where the chip cross-section and flow differ significantly from conventional turning, potentially lowering maximum forces and altering the distribution between the main, feed, and radial force components. Moreover, tangential turning can allow for the use of high feed rates without proportionally increasing the cutting load, offering the potential for higher productivity with controlled mechanical stresses.

The suitability of tangential turning for high-feed applications is of particular interest in modern manufacturing. High-feed machining generally aims to increase material removal rates by applying larger feeds per revolution while keeping depth of cut and cutting speed within ranges that preserve tool life [16,17]. However, in conventional turning, increasing feed rates often leads to an unbalanced rise in cutting forces and power consumption, which can exceed machine tool limits and cause rapid tool wear. Tangential turning, due to its altered chip formation and cutting geometry, may mitigate these negative effects, enabling higher feeds without the usual drawbacks. This makes it a potential technology for roughing operations and for applications where both high productivity and controlled force levels are required.

For high-strength alloyed steels such as 42CrMo4 (AISI 4140 equivalent), which is widely used in automotive,

aerospace, and general engineering applications, optimizing the turning process is of practical importance [18,19]. Its high strength, toughness, and wear resistance make it suitable for critical load-bearing components such as transmission shafts, crankshafts, and high-stress fasteners. However, these same properties also make it more challenging to machine, often resulting in higher cutting forces and rapid tool wear if cutting conditions are not carefully selected. Understanding and reducing the specific cutting forces when machining 42CrMo4 is therefore a matter of both economic and technical significance.

In this context, experimental studies that systematically vary key cutting parameters are necessary to characterize their effect on cutting forces and specific cutting forces in tangential turning. Among the available methodologies, the full factorial design of experiments (DOE) offers a thorough and efficient approach [20–22]. By considering all combinations of the selected factor levels – in this case, feed rate, depth of cut, and cutting speed – the method enables not only the identification of main effects but also the analysis of interaction effects between parameters. This provides a complete picture of how each factor influences the forces and whether certain parameter combinations yield synergistic or disadvantageous effects on specific cutting forces.

Applying a full factorial DOE to the tangential turning of 42CrMo4 steel allows for a structured investigation into the relationships between process parameters and force responses. Measuring cutting forces in the tangential, feed, and radial directions enables the calculation of corresponding specific cutting forces, which in turn allows for meaningful comparisons between conditions with different chip cross-sections. Such an approach is not only relevant for optimizing tangential turning in this material but also contributes to the broader understanding of how feed direction and chip geometry affect the mechanics of cutting.

The results of such studies have direct implications for process planning in industrial settings [23,24]. They can guide the selection of feeds, depths of cut, and cutting speeds that achieve the desired balance between productivity, tool life, and machine load capacity. Additionally, they can inform the design of tangential turning tools and inserts optimized for specific workpiece materials and performance targets. By quantifying the potential of tangential turning to reduce specific cutting forces at high feeds, these findings support its consideration as a viable alternative to conventional turning in the machining of alloy steels.

This work aims to experimentally investigate the effect of feed, depth of cut, and cutting speed on cutting forces and specific cutting forces in the tangential turning of 42CrMo4 steel shafts. Using a full factorial design of experiments, the study measures force components and calculates specific cutting forces for each case. The objective is to identify parameter combinations that minimize specific cutting forces while enabling high-feed operation, thereby contributing to both the scientific understanding and industrial application of tangential turning.

## 2. EXPERIMENTAL CONDITIONS AND METHODS

The experimental work was conducted to investigate the influence of cutting parameters on cutting forces and specific cutting forces in the tangential turning of 42CrMo4 alloyed steel shafts. The experiments were designed according to a full factorial scheme to systematically study the effects of cutting speed, feed per revolution, and depth of cut on the three principal cutting force components. The measured forces in tangential, radial, and axial directions were subsequently used to calculate specific cutting forces for each condition.

The turning tests were carried out on an EMAG VSC 400 DS hard machining center. This vertical spindle turning machine offers the rigidity and precision necessary for controlled measurement of cutting forces, while its high stiffness and dynamic stability help to minimize undesired vibrations that could affect force readings. The workpieces were securely clamped to ensure stable engagement between the tool and workpiece throughout each pass. The accuracy and repeatability of the machine tool provided a consistent basis for the comparative evaluation of the cutting parameters under study.

The cutting tool assembly consisted of an S117.0032.00 insert mounted in an H117.2530.4132 tool holder, both manufactured by HORN Cutting Tools Ltd., using MG12 grade insert material. This insert-holder combination was chosen for its suitability in high-feed tangential turning operations and its proven capability for machining hardened steels. The insert geometry (45° inclination angle) was selected to promote efficient chip formation while maintaining edge strength under high contact loads. The MG12 grade, designed for alloy steels, offers a combination of wear resistance and toughness required to withstand the higher mechanical and thermal loads generated when machining 42CrMo4 at both low and high cutting speeds.

The workpiece material was 42CrMo4 alloy steel (AISI 4140 equivalent), heat-treated to a hardness of 410 HV10. This steel is widely used for high-strength mechanical components, and its combination of high tensile strength, good toughness, and wear resistance makes it representative of industrial applications where turning performance is critical. The hardness level selected in this study represents a challenging yet realistic machining condition, making the results directly relevant to high-performance production environments. The shafts were pre-machined to 65 mm diameter and prepared to ensure consistent material properties and surface conditions before the experiments, thereby reducing variability in force measurement results.

Cutting force measurement was carried out using a Kistler 9257A three-component dynamometer, which is capable of simultaneously measuring the tangential (major cutting force –  $F_c$ ), radial (thrust force –  $F_p$ ), and axial (feed directional force –  $F_f$ ) force components with high sensitivity and accuracy. The dynamometer was rigidly mounted between the tool-holding fixture of the machine tool and the cutting tool to ensure that all force components were accurately transmitted and recorded without

interference. The sensor signals from the dynamometer were routed through Kistler 5011 charge amplifiers, which conditioned the signals for subsequent digital acquisition. The digitized signals were captured using a National Instruments NI-9215 analog input data acquisition module, which was installed in an NI cDAQ-9171 chassis. This modular data acquisition system provided reliable, high-speed sampling of the force signals, preserving the transient details of the cutting force variations. The data acquisition rate (1000 Hz) was selected to ensure that the recorded signals accurately represented the force behavior during the cutting process, avoiding aliasing effects or loss of high-frequency content. The acquisition and real-time monitoring of force signals were realized using NI LabVIEW software, which also allowed for data storage in a structured format suitable for post-processing and analysis.

The choice of cutting parameters followed a full factorial design of experiments approach, considering three factors—cutting speed, feed per revolution, and depth of cut—each at two levels. This resulted in a total of eight experimental conditions, which are summarized in Table 1, ensuring that all combinations of the selected parameter levels were tested.

**Table 1 – Experimental setups and the transformed values.**

Setup	1	2	3	4	5	6	7	8
Selected values of the setup parameters								
$v_c$ [m/min]	100	250	100	250	100	250	100	250
$f$ [mm/rev]	200	200	300	300	200	200	300	300
$a$ [mm]	0.1	0.1	0.1	0.1	0.2	0.2	0.2	0.2
Transformed values of the setup parameters								
$v_c'$ [-]	-1	1	-1	1	-1	1	-1	1
$f'$ [-]	-1	-1	1	1	-1	-1	1	1
$a'$ [-]	-1	-1	-1	-1	1	1	1	1

The cutting speeds investigated were 100 m/min (representing a lower-speed condition) and 250 m/min (representing a higher-speed condition). These values were chosen to reflect realistic production ranges for 42CrMo4 while providing a sufficient difference to capture the influence of cutting speed on both force magnitudes and specific cutting forces. The feed per revolution was set at 0.3 mm/rev and 0.6 mm/rev, corresponding to medium and high feed rates for tangential turning. These values were selected to examine how substantial changes in feed influence the chip cross-sectional area and, consequently, the cutting forces. Since tangential turning is generally capable of sustaining higher feed rates compared to conventional turning, the chosen range allows for observing potential advantages of this method under higher feed conditions. The depth of cut was varied between 0.1 mm and 0.2 mm. This range, while modest, was selected to investigate force sensitivity to changes in chip width without introducing excessive mechanical loads that could obscure the comparative influence of feed and cutting speed. Maintaining relatively small depths of cut also ensured stable engagement of the insert cutting edge, minimizing tool deflection and vibration.

For each experimental run, the workpiece was machined under the assigned combination of cutting parameters, and the cutting forces were continuously recorded. The measurement covered the steady-state portion of the cut, avoiding transient effects associated with tool entry and exit. The force signals were post-processed to remove any electrical noise and to extract representative average values for each force component. These averages were then normalized by the corresponding uncut chip cross-sectional area to obtain specific cutting forces for the tangential, radial, and axial directions. The uncut chip cross-sectional area ( $A_c$ ) was calculated from the product of feed per revolution ( $f$ ) and depth of cut ( $a_p$ ). For each condition, the specific cutting force in the tangential direction ( $k_c$ ) was computed as the ratio  $F_c/A_c$ , while similar expressions were used for the radial ( $k_r = F_r/A_c$ ) and axial ( $k_p = F_p/A_c$ ) directions. These values provided a basis for comparing cutting conditions on an equal basis, independent of variations in chip size.

This experimental arrangement provided a dataset for evaluating the influence of cutting speed, feed, and depth of cut on cutting forces and specific cutting forces in tangential turning of 42CrMo4 steel. The chosen methodology allows not only for the assessment of main parameter effects but also for the exploration of interaction effects inherent in the full factorial design, contributing to a comprehensive understanding of the cutting mechanics in this high-feed turning process. Equation 1 expresses the analyzed parameters through a polynomial model that combines the effects of cutting speed ( $v_c$ ), feed ( $f$ ), and depth of cut ( $a_p$ ), as well as their interaction terms. In this formulation, each constant ( $k_i$ ) represents the magnitude of influence associated with its corresponding variable or interaction.

$$y(v_c, f, a) = k_0 + k_1 v_c + k_2 f + k_3 a + k_{12} v_c f + k_{13} v_c a + k_{23} f a + k_{123} v_c f a \quad (1)$$

### 3. RESULTS

All planned cutting experiments were successfully completed according to the full factorial design. For each of the eight parameter combinations, the tangential (major cutting force –  $F_c$ ), axial (feed directional force –  $F_f$ ), and radial (thrust force –  $F_p$ ) components were measured using the dynamometer system. The recorded force signals were processed to obtain representative average values under steady-state cutting conditions.

**Table 2 – Force measurement and calculation results.**

Setup	1	2	3	4	5	6	7	8
$F_c$ [N]	245.2	204.0	345.7	304.5	426.4	388.2	717.3	558.7
$F_f$ [N]	231.1	279.4	275.9	398.1	282.6	553.5	492.7	590.2
$F_p$ [N]	71.9	72.9	115.6	128.5	147.9	138.4	296.9	347.4
$k_c$ [N/mm <sup>2</sup> ]	8175	6801	5762	5076	7107	6469	5978	4656
$k_f$ [N/mm <sup>2</sup> ]	7702	9314	4599	6636	4710	9225	4106	4918
$k_p$ [N/mm <sup>2</sup> ]	2397	2429	1927	2142	2465	2307	2474	2895

From these measured forces, the corresponding specific cutting forces were calculated in each principal direction

by normalizing with the uncut chip cross-sectional area ( $A_c$ ). Thus, for every experimental setup, six values were obtained: three measured force components ( $F_c, F_f, F_p$ ) and three calculated specific cutting forces ( $k_c, k_f, k_p$ ). The complete dataset for all eight experimental conditions is presented in Table 2.

Based on the experimental results, polynomial regression analysis was applied to derive predictive equations for the forces and specific cutting forces as functions of feed per revolution ( $f$ ), cutting speed ( $v_c$ ), and depth of cut ( $a_p$ ), including interaction terms. The relationship describing the major cutting force is expressed in Equation 2.

$$F_c(v_c, f, a) = ((-26.76a + 2.678)f + 8.224a - 1.098)v_c + (9026a - 568)f - 915.2a + 264 \quad (2)$$

The dependence of the feed directional force on the studied parameters is modelled in Equation 3.

$$F_f(v_c, f, a) = ((-54.96a + 7.137)f + 31.32a - 3.302)v_c + (11000a - 1115)f - 4269.a + 630 \quad (3)$$

Equation 4 presents the derived model for predicting the value of thrust force.

$$F_p(v_c, f, a) = ((10.7a - 0.8062)f - 3.907a + -0.3177)v_c + (2435a - 124.3)f + 98.9a + 25.7 \quad (4)$$

The corresponding formulation for the specific cutting force in the tangential direction is given in Equation 5.

$$k_c(v_c, f, a) = ((-304.9a + 45.78)f + 140.6a - 27.80)v_c + (73310a - 16910)f - 37590a + 15720 \quad (5)$$

Equation 6 details the calculated expression for the specific cutting force in the axial direction.

$$k_f(v_c, f, a) = ((-917.1a + 101.2)f + 468.5a - 38.94)v_c + (175000a - 28800)f - 101800a + 20190 \quad (6)$$

Finally, the mathematical relationship for the specific cutting force in the radial direction is summarized in Equation 7.

$$k_p(v_c, f, a) = ((88.24a - 4.771)f - 39.13a + 2.910)v_c + (7110.a - 2684)f - 188.9a + 2987 \quad (7)$$

These equations quantify the influence of each cutting parameter and their interactions on both the absolute and specific cutting forces, providing a basis for predicting cutting performance under varying tangential turning conditions.

#### 4. DISCUSSION

The analysis of the experimental results is based on the polynomial regression models derived in Equations 2–7 and the trend visualizations presented in Figures 1–6. Each figure illustrates the relationship between the investigated cutting parameters – cutting speed ( $v_c$ ), feed per revolution ( $f$ ), and depth of cut ( $a_p$ ) – and the respective measured or calculated force component. The following discuss the influence of these parameters on each force and specific force component individually, enabling a clear understanding of their effects in tangential turning of 42CrMo4 steel.

The major cutting force ( $F_c$ ) shows clear and consistent sensitivity to both feed and depth of cut. Increasing the feed from 0.3 mm/rev to 0.6 mm/rev while keeping the depth of cut constant at 0.1 mm results in an increase in  $F_c$  from 245.24 N to 345.69 N at 100 m/min (a 41% increase), and from 204.03 N to 304.54 N at 250 m/min (a 49% increase). When the depth of cut is doubled from 0.1 mm to 0.2 mm, a larger effect is observed. At the lower feed (0.3 mm/rev),  $F_c$  rises from 245.24 N to 426.39 N at 100 m/min, representing a 74% increase, and from 204.03 N to 388.15 N at 250 m/min (a 90% increase).

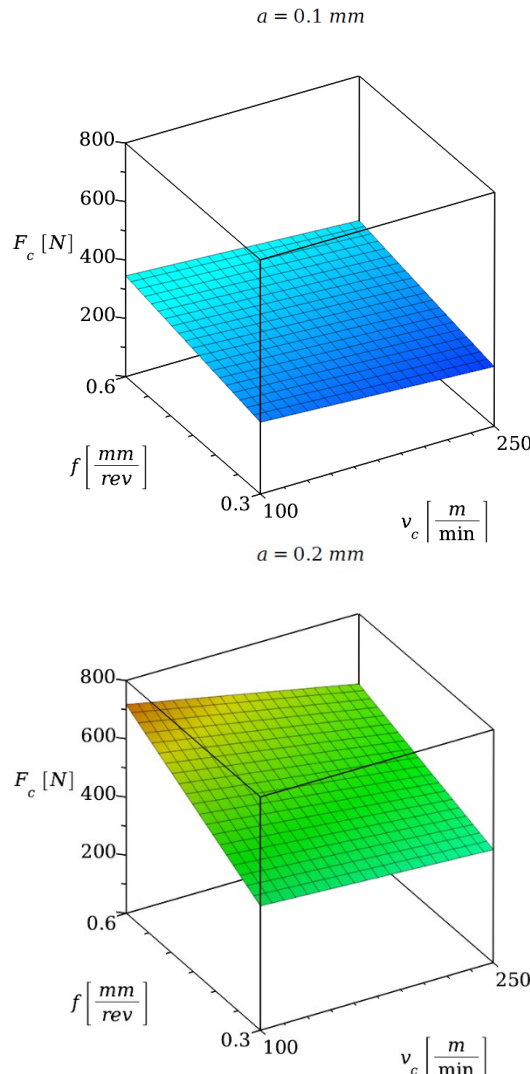


Fig. 1 The major cutting force in function of the studied variables

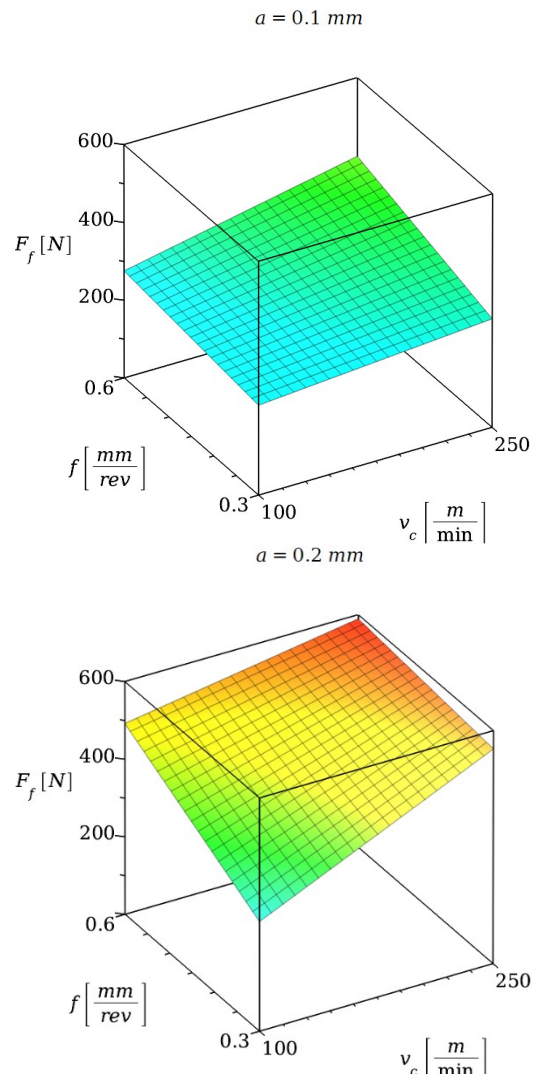


Fig. 2 The feed force in function of the studied variables

Under the highest-load condition ( $f = 0.6 \text{ mm/rev}$ ,  $a_p = 0.2 \text{ mm}$ ),  $F_c$  reaches its maximum value of 717.31 N at 100 m/min, which then drops to 558.73 N at 250 m/min. This corresponds to a 22% reduction, suggesting that higher cutting speed contributes to force reduction—likely due to thermal softening of the work material and improved chip formation. Overall,  $F_c$  increases with both feed and depth of cut, while increasing cutting speed tends to reduce the required force. These trends are represented in Figure 1 and Equation 2.

The feed directional force ( $F_f$ ) shows a complex interaction between the cutting parameters, with significant sensitivity to cutting speed. At a depth of cut of 0.1 mm and increasing feed from 0.3 mm/rev to 0.6 mm/rev,  $F_f$  rises from 231.06 N to 275.95 N at 100 m/min (a 19% increase) but shows a much larger jump from 279.42 N to 398.15 N at 250 m/min (a 42% increase). Doubling the depth of cut at 0.3 mm/rev leads to increases from 231.06 N to 282.63 N at 100 m/min (22%) and from 279.42 N to 553.48 N at 250 m/min, almost doubling the force. Notably, the largest increase is seen when both feed and depth of cut are increased together: at  $f = 0.6 \text{ mm/rev}$  and  $a_p = 0.2 \text{ mm}$ ,  $F_f$  increases from 492.72 N to 590.16 N as cutting speed increases,

contrary to expectations based on  $F_c$  trends. This 20% rise suggests that in tangential turning, higher cutting speed may increase axial resistance under certain chip geometries. The overall trend indicates that  $F_f$  is more sensitive to increases in cutting speed than  $F_c$ , especially at higher chip cross-sections. This complex behaviour is shown in the surface plots shown in Figure 2 and in the interaction terms of Equation 3.

The thrust force ( $F_p$ ) increases steadily with both feed and depth of cut, but unlike  $F_c$  and  $F_f$ , it also increases with cutting speed in all tested configurations. For instance, at  $f = 0.3 \text{ mm/rev}$  and  $a_p = 0.1 \text{ mm}$ ,  $F_p$  increases slightly from 71.92 N to 72.88 N as cutting speed increases from 100 m/min to 250 m/min. At  $f = 0.6 \text{ mm/rev}$  and the same depth,  $F_p$  rises from 115.64 N to 128.52 N (a 11% increase). The most significant increases occur at the highest depth of cut. At  $a_p = 0.2 \text{ mm}$  and  $f = 0.3 \text{ mm/rev}$ , the thrust force increases from 147.92 N to 138.43 N (a minor decrease), while at  $f = 0.6 \text{ mm/rev}$ , the force rises sharply from 296.85 N to 347.44 N – a 17% increase. Compared to  $F_c$  and  $F_f$ ,  $F_p$  demonstrates a more linear and consistent growth with chip cross-sectional area, and its increasing trend with cutting speed could be linked to increased ploughing or deflection effects at higher speeds.

$$a = 0.1 \text{ mm}$$

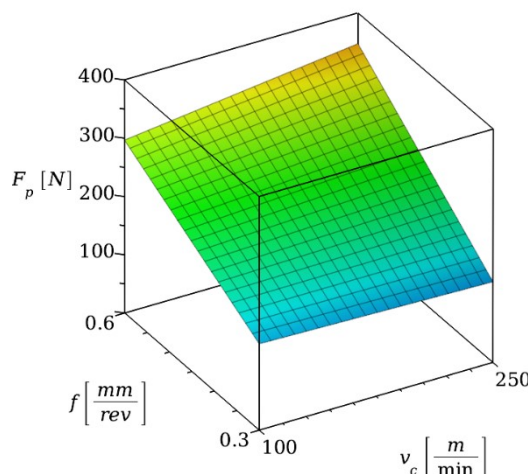
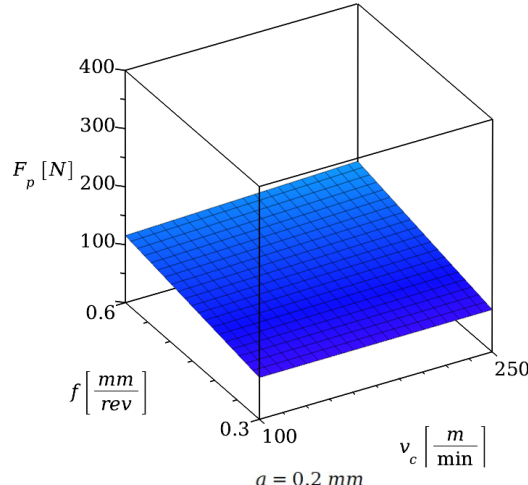


Fig. 3 The thrust force in function of the studied variables

These effects are likely amplified in the radial direction due to the tool orientation in tangential turning. Figure 3 visualizes these interactions, while Equation 4 quantifies the relationships.

The specific cutting force in the tangential direction ( $k_c$ ) shows an inverse relationship with increasing chip cross-sectional area. At  $a_p = 0.1 \text{ mm}$  and  $f = 0.3 \text{ mm/rev}$  ( $A_c = 0.03 \text{ mm}^2$ ),  $k_c$  is 8175 N/mm<sup>2</sup> at 100 m/min. When cutting speed is increased to 250 m/min,  $k_c$  drops to 6801 N/mm<sup>2</sup> – a 17% decrease. When feed is doubled to 0.6 mm/rev ( $A_c = 0.06 \text{ mm}^2$ ),  $k_c$  decreases further to 5762 N/mm<sup>2</sup> and 5076 N/mm<sup>2</sup> at 100 and 250 m/min respectively. These changes represent a 30–37% reduction compared to the lowest-chip-section case. At the highest chip area ( $A_c = 0.12 \text{ mm}^2$ ),  $k_c$  reaches its lowest values of 5978 N/mm<sup>2</sup> (100 m/min) and 4656 N/mm<sup>2</sup> (250 m/min). This decrease – 43% from the initial maximum – confirms that increasing chip cross-section leads to better material removal efficiency. The decrease with cutting speed is also consistent across all chip sizes. These results support the known trend that specific cutting forces diminish as more material is removed per unit time, due to improved thermal softening and reduced strain hardening per unit volume. The effects are shown in Figure 4 and in Equation 5.

$$a = 0.1 \text{ mm}$$

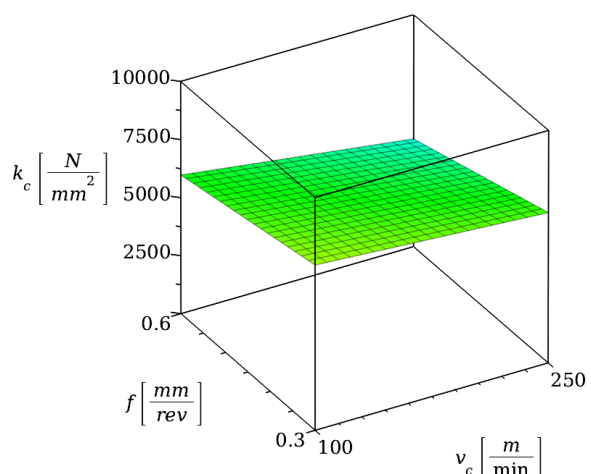
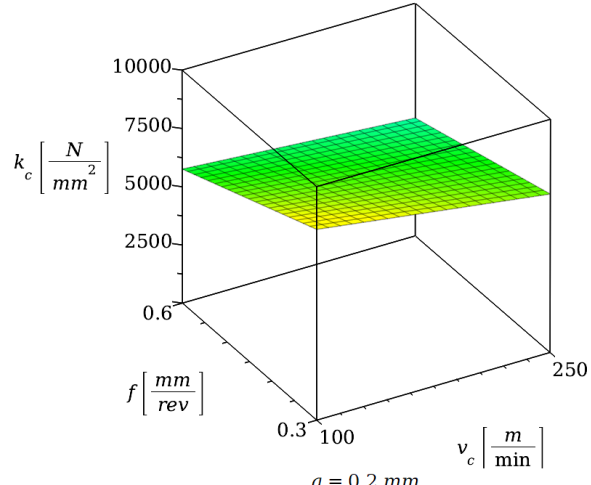


Fig. 4 The specific major cutting force in function of the variables

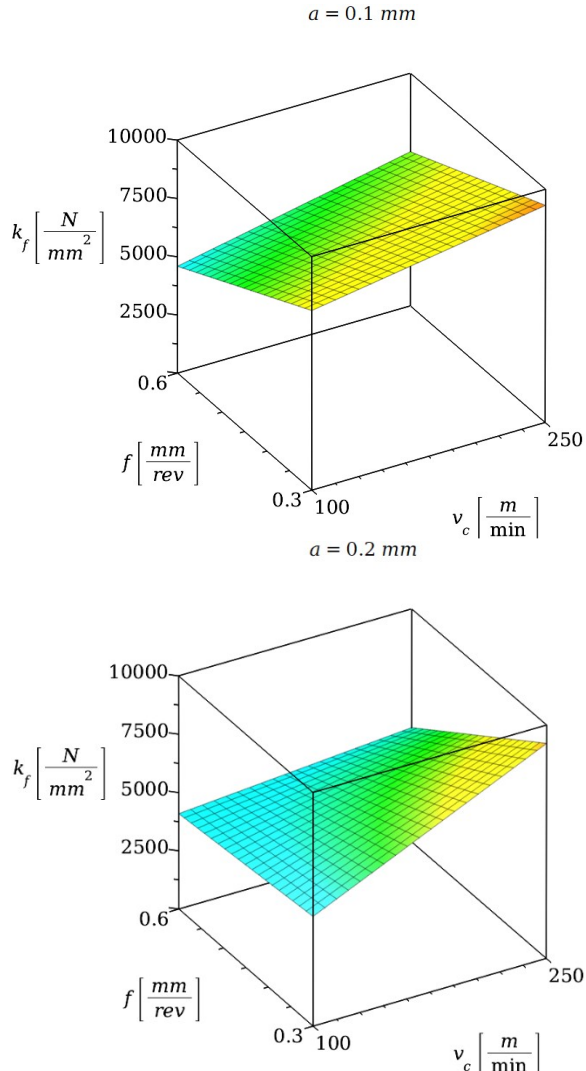


Fig. 5 The specific feed force in function of the studied variables

The specific cutting force in the axial direction ( $k_f$ ) also decreases with increasing chip area, although not as consistent as  $k_c$ . At  $A_c = 0.03 \text{ mm}^2$ ,  $k_f$  is  $7702 \text{ N/mm}^2$  and  $9314 \text{ N/mm}^2$  for 100 and 250 m/min respectively, with an unusual increase of 21% at higher speed. As feed increases to  $0.6 \text{ mm/rev}$  ( $A_c = 0.06 \text{ mm}^2$ ),  $k_f$  drops to  $4599 \text{ N/mm}^2$  and  $6636 \text{ N/mm}^2$ , reflecting reductions of 40% and 29% compared to the lower chip section. The most pronounced reduction is observed at the largest chip area ( $A_c = 0.12 \text{ mm}^2$ ), where  $k_f$  drops to  $4106 \text{ N/mm}^2$  (100 m/min) and  $4918 \text{ N/mm}^2$  (250 m/min). Compared to the initial value at 250 m/min, this represents a 47% reduction. The cutting speed effect is more complex: in some cases, increasing  $v_c$  leads to higher  $k_f$  values, particularly at lower feeds and depths, but this trend diminishes at higher material removal rates. These variations suggest a more sensitive axial response to dynamic effects such as chip removal or tool deflection under high feed rates. These behaviors are visualized in Figure 5 and modelled by Equation 6.

The specific cutting force in the radial (thrust) direction ( $k_p$ ) shows the least predictable pattern among the specific force components. At  $A_c = 0.03 \text{ mm}^2$ ,  $k_p$  is  $2397 \text{ N/mm}^2$  at 100 m/min and increases slightly to  $2429 \text{ N/mm}^2$  at 250

m/min. When  $A_c$  increases to  $0.06 \text{ mm}^2$ ,  $k_p$  initially decreases to  $1927 \text{ N/mm}^2$  (100 m/min) but increases again to  $2142 \text{ N/mm}^2$  (250 m/min), suggesting a partial reversal of the expected trend. At  $A_c = 0.12 \text{ mm}^2$ ,  $k_p$  rises to  $2474 \text{ N/mm}^2$  and  $2895 \text{ N/mm}^2$  at 100 and 250 m/min respectively. The increase from  $1927 \text{ N/mm}^2$  to  $2895 \text{ N/mm}^2$  represents a 50% rise with cutting speed and chip cross-section. This contrasts with the decreasing trends of  $k_c$  and  $k_f$ , suggesting that radial force behavior may be governed by additional factors such as chip curling, side flow, or tool deflection geometry specific to tangential turning. The higher  $k_p$  values at larger chip areas might also indicate increased radial tool load due to side contact. These nonlinear interactions are shown in Figure 6 and captured by the regression model in Equation 7.

When analyzing the combined behavior of the measured force components and their corresponding specific values, a coherent pattern emerges that highlights the complex interactions between the cutting parameters and force responses in tangential turning of 42CrMo4 steel. Among the measured forces, the major cutting force ( $F_c$ ) consistently dominates in magnitude, followed by the feed directional force ( $F_f$ ) and the thrust force ( $F_p$ ).

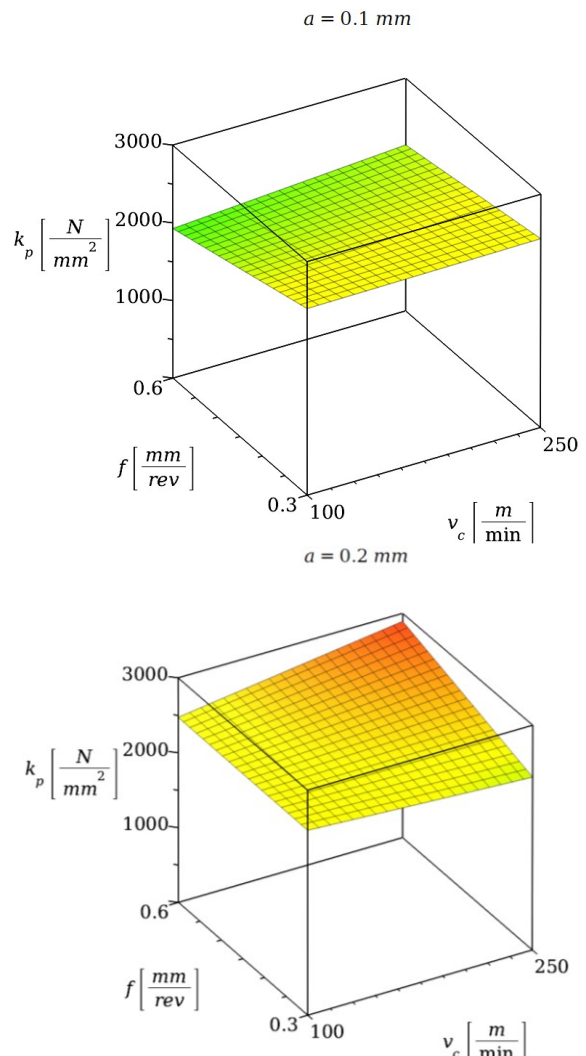


Fig. 6 The specific thrust force in function of the studied variables

This hierarchy reflects the mechanical load distribution characteristic to the tool orientation and chip formation mechanism in tangential turning.

Feed per revolution and depth of cut apply the strongest influence on absolute force values, with both parameters contributing proportionally to the increase in the uncut chip cross-sectional area ( $A_c$ ). Doubling either feed or depth of cut led to significant increases in  $F_c$ ,  $F_f$ , and  $F_p$  – typically ranging between 40% and 90%, depending on the combination. However, cutting speed ( $v_c$ ) introduced more complex effects: in most cases, higher cutting speed caused a decrease in the measured forces, particularly in  $F_c$ , suggesting a thermal softening effect and improved chip breakability at increased speeds.

When the force values are normalized to obtain the specific cutting forces ( $k_c$ ,  $k_f$ ,  $k_p$ ), the influence of chip geometry becomes more evident.  $k_c$  and  $k_f$  both demonstrate a strong inverse relationship with chip cross-sectional area: at higher feeds and depths, the material removal becomes more efficient, resulting in specific force reductions of 30–50%. However,  $k_p$  deviates from this trend – exhibiting non-monotonic behavior and even increasing in some high-feed and high-speed scenarios. This suggests that radial force generation is more sensitive to secondary effects, such as tool side engagement, chip flow direction, or lateral tool deflection.

Overall, the combined analysis shows that  $F_c$  and  $k_c$  serve as reliable indicators of overall cutting efficiency, while  $F_f$  and  $F_p$  – along with their specific counterparts – reveal deeper mechanical interactions, particularly under varying chip geometry and thermal conditions. The divergence observed in  $k_p$  also underlines the importance of considering all three force components, especially in high-feed turning strategies where radial loads may become critical for tool stability and surface quality.

## 5. CONCLUSIONS

This study investigated the cutting force characteristics in tangential turning of 42CrMo4 alloy steel using a full factorial experimental design. The primary objective was to evaluate how variations in feed per revolution, depth of cut, and cutting speed influence the three principal force components – tangential ( $F_c$ ), axial ( $F_f$ ), and radial ( $F_p$ ) – and their corresponding specific cutting forces ( $k_c$ ,  $k_f$ ,  $k_p$ ). The motivation behind this research was to enhance the understanding of process mechanics in high-feed turning operations and support the development of more efficient and stable cutting strategies for hard-to-machine steels.

The experiments were conducted on an EMAG VSC 400 DS hard turning center using HORN tooling with MG12-grade inserts. Cutting forces were measured using a Kistler 9257A dynamometer system, and data acquisition was handled through a NI-based system running LabVIEW. For each of the eight experimental setups defined by the full factorial parameter combinations, six parameters were evaluated: three absolute force values and three specific force values. These were analyzed using polynomial regression models and visualized in Figures.

The results showed that both feed and depth of cut significantly affect the magnitude of cutting forces, primarily due to their direct influence on the chip cross-sectional area. Cutting speed generally reduced the force values, particularly  $F_c$ , suggesting thermal softening effects. Specific cutting forces ( $k_c$ ,  $k_f$ ) demonstrated a clear decreasing trend with increasing material removal rate, reflecting improved energy efficiency at higher feeds and depths. In contrast,  $k_p$  exhibited a more irregular pattern, occasionally increasing with cutting speed or chip load – pointing to possible secondary effects related to tool side engagement and chip flow.

The key findings of this study are the following:

- (1) The tangential turning of 42CrMo4 enables stable machining even under high feed and low depth conditions, with reduced  $k_c$  values at increased chip loads.
- (2) Specific forces reveal efficiency gains not evident from absolute forces alone, especially in  $k_c$  and  $k_f$  trends.
- (3) The radial force behavior ( $k_p$ ) is controlled by complex interactions beyond chip geometry, emphasizing the need for its separate evaluation in high-feed turning.

These contributions support improved force prediction, tool design, and process optimization in high-performance turning applications.

## ACKNOWLEDGEMENTS

Supported by the University Research Scholarship Program of the Ministry for Culture and Innovation from the source of the National Research, Development and Innovation fund. Contract identifier: TNI/1648-64/2024. Scholarship identifier: EKÖP-24-4-II-15.

## REFERENCES

- [1] Chuangwen, X., Jianming, D., Yuzhen, C., Huaiyuan, L., Zhicheng, S., & Jing, X. (2018). The relationships between cutting parameters, tool wear, cutting force and vibration. *Advances in Mechanical Engineering*, 10(1): 1–12. <https://doi.org/10.1177/1687814017750434>
- [2] Mohamed, A., Hassan, M., M'Saoubi, R., & Attia, H. (2022). Tool Condition Monitoring for High-Performance Machining Systems—A review. *Sensors*, 22(6): 2206. <https://doi.org/10.3390/s22062206>
- [3] Felhő, C., & Namboodri, T. (2024). Statistical analysis of cutting force and vibration in turning X5CrNi18-10 steel. *Applied Sciences*, 15(1): 54. <https://doi.org/10.3390/app15010054>
- [4] Pálmai, Z., Kundrák, J., Felhő, C., & Makkai, T. (2024). Investigation of the transient change of the cutting force during the milling of C45 and X5CrNi18-10 steel taking into account the dynamics of the electro-mechanical measuring system. *The International Journal of Advanced Manufacturing Technology*, 133(1–2): 163–182. <https://doi.org/10.1007/s00170-024-13640-6>

[5] Felhő, C. (2023). Analysis of the effect of varying the cutting ratio on force components and surface roughness in face milling. *Cutting & Tools in Technological System*, 99: 3–11. <https://doi.org/10.20998/2078-7405.2023.99.01>

[6] Jayaram, S., Kapoor, S., & DeVor, R. (2001). Estimation of the specific cutting pressures for mechanistic cutting force models. *International Journal of Machine Tools and Manufacture*, 41(2): 265–281. [https://doi.org/10.1016/s0890-6955\(00\)00076-6](https://doi.org/10.1016/s0890-6955(00)00076-6)

[7] Kundrák, J., Karpuschewski, B., Pálmai, Z., Felhő, C., Makkai, T., & Borysenko, D. (2020). The energetic characteristics of milling with changing cross-section in the definition of specific cutting force by FEM method. *CIRP Journal of Manufacturing Science and Technology*, 32: 61–69. <https://doi.org/10.1016/j.cirpj.2020.11.006>

[8] Denkena, B., Vehmeyer, J., Niederwestberg, D., & Maaß, P. (2014). Identification of the specific cutting force for geometrically defined cutting edges and varying cutting conditions. *International Journal of Machine Tools and Manufacture*, 82–83: 42–49. <https://doi.org/10.1016/j.ijmachtools.2014.03.009>

[9] Yun, W., & Cho, D. (2001). Accurate 3-D cutting force prediction using cutting condition independent coefficients in end milling. *International Journal of Machine Tools and Manufacture*, 41(4): 463–478. [https://doi.org/10.1016/s0890-6955\(00\)00097-3](https://doi.org/10.1016/s0890-6955(00)00097-3)

[10] Mukherjee, I., & Ray, P. K. (2006). A review of optimization techniques in metal cutting processes. *Computers & Industrial Engineering*, 50(1–2): 15–34. <https://doi.org/10.1016/j.cie.2005.10.001>

[11] Yusup, N., Zain, A. M., & Hashim, S. Z. M. (2012). Evolutionary techniques in optimizing machining parameters: Review and recent applications (2007–2011). *Expert Systems with Applications*, 39(10): 9909–9927. <https://doi.org/10.1016/j.eswa.2012.02.109>

[12] Cui, X., Zhao, B., Jiao, F., & Zheng, J. (2015). Chip formation and its effects on cutting force, tool temperature, tool stress, and cutting edge wear in high- and ultra-high-speed milling. *The International Journal of Advanced Manufacturing Technology*, 83(1–4): 55–65. <https://doi.org/10.1007/s00170-015-7539-7>

[13] Becze, C., & Elbestawi, M. (2002). A chip formation based analytic force model for oblique cutting. *International Journal of Machine Tools and Manufacture*, 42(4): 529–538. [https://doi.org/10.1016/s0890-6955\(01\)00129-8](https://doi.org/10.1016/s0890-6955(01)00129-8)

[14] Schubert, A., Zhang, R., & Steinert, P. (2013). Manufacturing of twist-free surfaces by hard turning. *Procedia CIRP*, 7: 294–298. <https://doi.org/10.1016/j.procir.2013.05.050>

[15] Sztankovics, I. (2024). Analytical determination of high-feed turning procedures by the application of constructive geometric modeling. *FME Transactions*, 52(2): 173–185. <https://doi.org/10.5937/fme2402173s>

[16] Barcelos, M., De Almeida, D., Tusset, F., & Scheuer, C. (2024). Performance analysis of conventional and high-feed turning tools in machining the thermally affected zone after plasma arc cutting of low carbon manganese-alloyed steel. *Journal of Manufacturing Processes*, 115: 18–39. <https://doi.org/10.1016/j.jmapro.2024.01.088>

[17] Khan, S. A., Ahmad, M. A., Saleem, M. Q., Ghulam, Z., & Qureshi, M. A. M. (2016). High-feed turning of AISI D2 tool steel using multi-radii tool inserts: Tool life, material removed, and workpiece surface integrity evaluation. *Materials and Manufacturing Processes*, 32(6): 670–677. <https://doi.org/10.1080/10426914.2016.1232815>

[18] Xu, Q., Zhao, J., & Ai, X. (2017). Cutting performance of tools made of different materials in the machining of 42CrMo4 high-strength steel: A comparative study. *The International Journal of Advanced Manufacturing Technology*, 93(5–8): 2061–2069. <https://doi.org/10.1007/s00170-017-0666-6>

[19] Makhesana, M. A., Baravaliya, J. A., Parmar, R. J., Mawandiya, B. K., & Patel, K. M. (2021). Machinability improvement and sustainability assessment during machining of AISI 4140 using vegetable oil-based MQL. *Journal of the Brazilian Society of Mechanical Sciences and Engineering*, 43(12): 1–15. <https://doi.org/10.1007/s40430-021-03256-2>

[20] Kleijnen, J. P. (2008). Design of experiments: Overview. *2008 Winter Simulation Conference*, 479–488. <https://doi.org/10.1109/wsc.2008.4736103>

[21] Ferencsik, V. (2024). FEM investigation of the roughness and residual stress of diamond burnished surface. *Journal of Experimental and Theoretical Analyses*, 2(4): 80–90. <https://doi.org/10.3390/jeta2040007>

[22] Smolnicki, S., & Varga, G. (2025). Analysis of surface roughness of diamond-burnished surfaces using Kraljic matrices and experimental design. *Applied Sciences*, 15(14): 8025. <https://doi.org/10.3390/app15148025>

[23] Sevella, V., Ali, A., Abdelhadi, A., & Alkhaleefah, A. (2025). Data-driven optimization of CNC manufacturing using simulation and DOE techniques. *Applied Sciences*, 15(14): 7637. <https://doi.org/10.3390/app15147637>

[24] Aleksić, A., Sekulić, M., Gostimirović, M., Rodić, D., Savković, B., & Antić, A. (2021). Effect of cutting parameters on cutting forces in turning of CPM 10V steel. *Journal of Production Engineering*, 24(2): 5–8. <https://doi.org/10.24867/jpe-2021-02-005>